Influence of Mixed Substituents on the Macrocyclic Ring Distortions of Free Base Porphyrins and Their Metal Complexes

3 AUTHORS:

Bhyrappa Puttaiah
Indian Institute of Technology Madras
52 PUBLICATIONS **1,559** CITATIONS

Chellaiah Arunkumar
National Institute of Technology Calicut
28 PUBLICATIONS **120** CITATIONS

Babu Varghese
Indian Institute of Technology Madras
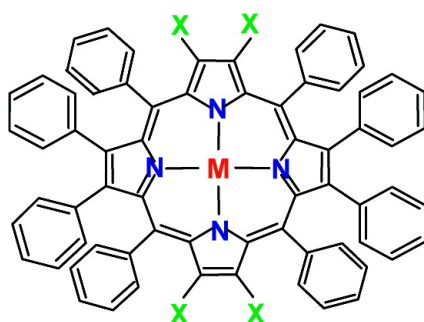**227** PUBLICATIONS **2,384** CITATIONS

Article

Influence of Mixed Substituents on the Macrocyclic Ring Distortions of Free Base Porphyrins and Their Metal Complexes

P. Bhyrappa, C. Arunkumar, and B. Varghese

M = 2H, X = CN, Cl, Br
M = Ni(II), X = CN
M = Zn(II), X = Cl

More About This Article

Additional resources and features associated with this article are available within the HTML version:

- Supporting Information
- Access to high resolution figures
- Links to articles and content related to this article
- Copyright permission to reproduce figures and/or text from this article

View the Full Text HTML

Inorganic Chemistry

·Article

Influence of Mixed Substituents on the Macrocyclic Ring Distortions of Free Base Porphyrins and Their Metal Complexes

P. Bhyrappa,* C. Arunkumar, and B. Varghese

Department of Chemistry, Indian Institute of Technology Madras, Chennai 600 036, India

Crystal structures of a series of free base porphyrins, 2,3,12,13-tetra(cyano/chloro/bromo)-5,7,8,10,15,17,18,20-octaphenylporphyrin solvates [$H_2(TPP(Ph)_4(CN)_4) \cdot 3(C_2H_4Cl_2)$, $H_2(TPP(Ph)_4Cl_4) \cdot 2(CH_3OH)$, and $H_2(TPP(Ph)_4Br_4) \cdot 2THF \cdot 1.5(CH_3OH)$], were determined to examine the influence of mixed antipodal β-pyrrole substitution on the stereochemistry of the porphyrin macrocycle. Nonplanarity of the porphyrin skeleton increases with an increase in size of the X group at the β-pyrrole positions, and the root-mean-square deviation of the core atoms follows the order CN (0.508 Å) < Cl (0.687 Å) < Br (0.792 Å). The normal-coordinate decomposition analysis of the free-base structures shows dramatic substituent- (X-)dependent out-of-plane distortions featuring saddling combined with a ruffled conformation in $H_2(TPP(Ph)_4(CN)_4)$, while it is predominantly saddled geometry in $H_2(TPP(Ph)_4X_4)$ (X = Cl, Br) structures. For $H_2(TPP(Ph)_4X_4)$ (X = Cl, Br) structures, the core elongation is along the antipodal pyrroles bearing halogen groups, and in the case of the $H_2(TPP(Ph)_4(CN)_4)$ structure, it is along the other antipodal pyrroles with phenyl groups. However, the average core, N···N separation along the transannular pyrrole direction follows the trend $H_2(TPP(Ph)_4(CN)_4)$ (4.134(4) Å) < $H_2(TPP(Ph)_4Cl_4)$ (4.184(5) Å) < $H_2(TPP(Ph)_4Br_4)$ (4.205(5) Å). The bond lengths of the 24-atom core are comparable, but its bond angles showed significant differences along the antipodal direction bearing β-pyrrole with X groups when compared to the other transannular pyrrole direction. The four-nitrogen porphyrin core (N_4H_2) exhibited weak intramolecular hydrogen bonding and also intermolecular interactions. Interestingly, $H_2(TPP(Ph)_4Cl_4) \cdot 2(CH_3OH)$ shows an extended chain structure involving hydrogen-bonding interactions between the CH₃OH···OHCH₃ (O···O) and CH₃OH···core (N_4H_2) interactions. The nonplanar geometry of these free base porphyrin rings suggests a more predominant influence of steric crowding of the peripheral substituents rather than intermolecular interactions. The four-coordinated $Ni(TPP(Ph)_4(CN)_4) \cdot C_6H_{14} \cdot 0.5(C_2H_4Cl_2)$ complex shows an enhanced ruffling of the macrocycle along with the saddled conformation relative to more saddle-shaped $H_2(TPP(Ph)_4(CN)_4) \cdot 3(C_2H_4Cl_2)$ structure. The crystal structure of the $Zn(TPP(Ph)_4Cl_4)(Py) \cdot (C_2H_4Cl_2)$ complex features distorted square-pyramidal geometry with the reduction in the nonplanarity of the core in contrast to its free base porphyrin structure. Normal-coordinate-decomposition analysis for the out-of-plane displacement of the core atoms in the $Ni(TPP(Ph)_4(CN)_4)$ structure showed enhanced ruffling combined with saddling of the macrocycle while $Zn(TPP(Ph)_4Cl_4)(Py)$ exhibited mainly saddling when compared to their corresponding free base porphyrin structures. The nonplanar distortion in the $Ni(TPP(Ph)_4(CN)_4) \cdot (C_6H_{14}) \cdot 0.5(C_2H_4Cl_2)$ complex indicates that the contracted porphyrin core and the weak intermolecular interactions are responsible for the nonplanar geometry of the macrocyclic ring.

Introduction

Nonplanar conformations of tetrapyrrole pigments, in particular, influence the biological functions of various porphyrinoids in metalloproteins and have led to the synthesis of a wide range of sterically crowded, diverse porphyrins.[1−8] The presence of peripheral substituents produces new types of porphyrin chromophores with significantly altered physicochemical properties that arise from the conformational

---

* To whom correspondence should be addressed. E-mail: pbhyrappa@hotmail.com.

(1) Senge, M. O. In *The Porphyrin Handbook*; Kadish, K. M., Smith, K. M., Guilard, R., Eds.; Academic Press: New York, 2000; Vol. 1, p 239, and references therein.

distortions of the macrocycle.[9−32] Shelnutt and co-workers[2] have examined the stereochemistry of the heme centers in many hemeproteins and synthetic porphyrins with differing conformational features. An increase in the number of substituents enhances the steric crowding and thus induces enhanced steric repulsive interactions among the peripheral substituents, leading to the nonplanarity of the macrocycle.[1,33−44] High-valent metalloperhaloporphyrins serve as robust catalysts for the oxidative transformation of organic substrates.[45−51] The robust nature of the catalysts has been attributed to the stabilization of the highest-occupied π-molecular orbitals.[52,53] Unlike planar porphyrins, nonplanarity features disposition of the core nitrogen atoms above and below the faces of the macrocycle and produces dramatic solvent-dependent optical spectral properties.[54,55] In addition, nonplanar free base porphyrins exhibited facile metal insertion reactions.[56−58]

Another class of *meso*-tetraphenylporphyrins with electron-donor and electron-withdrawing groups at the β-pyrrole positions has also been reported by a few research

(2) (a) Shelnutt, J. A.; Song, X.-Z.; Ma, J.-G.; Jia, S.-L.; Jentzen, W.; Medforth, C. J. *Chem. Soc. Rev.* **1998**, *27*, 31, and references therein. (b) Shelnutt, J. A. In *The Porphyrin Handbook*; Kadish, K. M., Smith, K. M., Guilard, R., Eds.; Academic Press: New York, 2000; Vol. 7; p 167. (c) Jentzen, W.; Song, X.-Z.; Shelnutt, J. A. *J. Phys. Chem. B* **1997**, *101*, 1684. (d) Haddad, R. E.; Gazeau, S.; Pecaut, J.; Marchon, J.-C.; Medforth, C. J.; Shelnutt, J. A. *J. Am. Chem. Soc.* **2003**, *125*, 1253. (e) Ravikanth, M.; Chandrashekar, T. K. *Struct. Bonding (Berlin)*; Springer: Berlin, 1995; Vol. 82, p 107.

(3) Sparks, L. D.; Medforth, C. J.; Park, M.-S.; Chamberlain, J. R.; Ondrias, M. R.; Senge, M. O.; Smith, K. M.; Shelnutt, J. A. *J. Am. Chem. Soc.* **1993**, *115*, 581.

(4) Renner, M. W.; Furenlid, L. R.; Barkigia, K. M.; Forman, A.; Shim, H.-K.; Smith, K. M.; Fajer, J. *J. Am. Chem. Soc.* **1991**, *113*, 6891.

(5) Furenlid, L. R.; Renner, M. W.; Fajer, J. *J. Am. Chem. Soc.* **1990**, *112*, 8987.

(6) Shelnutt, J. A.; Medforth, C. J.; Berber, M. D.; Barkigia, K. M.; Smith, K. M. *J. Am. Chem. Soc.* **1991**, *113*, 4077.

(7) Senge, M. O.; Medforth, C. J.; Sparks, L. D.; Shelnutt, J. A.; Smith, K. M. *Inorg. Chem.* **1993**, *32*, 1716.

(8) Renner, M. W.; Barkigia, K. M.; Zhang, Y.; Medforth, C. J.; Smith, K. M.; Fajer, J. *J. Am. Chem. Soc.* **1994**, *116*, 8582.

(9) Gentemann, S.; Nelson, N. Y.; Jaquinod, L.; Nurco, D. J.; Leung, S. H.; Medforth, C. J.; Smith, K. M.; Fajer, J.; Holten, D. *J. Phys. Chem. B* **1997**, *101*, 1247.

(10) Drain, C. M.; Kirmaier, C.; Medforth, C. J.; Nurco, D. J.; Smith, K. M.; Holten, D. *J. Phys. Chem.* **1996**, *100*, 11984.

(11) Gentemann, S.; Leung, S. H.; Smith, K. M.; Fajer, J.; Holten, D. *J. Phys. Chem.* **1995**, *99*, 4330.

(12) Gentemann, S.; Medforth, C. J.; Forsyth, T. P.; Nurco, D. J.; Smith, K. M.; Fajer, J.; Holten, D. *J. Am. Chem. Soc.* **1994**, *116*, 7363.

(13) Ozette, K.; Leduc, P.; Palacio, M.; Bartoli, J.-F.; Barkigia, K. M.; Fajer, J.; Battioni, P.; Mansuy, D. *J. Am. Chem. Soc.* **1997**, *119*, 6442.

(14) Renner, M. W.; Barkigia, K. M.; Melamed, D.; Smith, K. M.; Fajer, J. *Inorg. Chem.* **1996**, *35*, 5120.

(15) Ochsenbein, P.; Ayougou, K.; Mandon, D.; Fischer, J.; Weiss, R.; Austin, R. N.; Jayaraj, K.; Gold, A.; Terner, J.; Fajer, J. *Angew. Chem., Int. Ed. Engl.* **1994**, *33*, 348.

(16) Barkigia, K. M.; Renner, M. W.; Furenlid, L. R.; Medforth, C. J.; Smith, K. M.; Fajer, J. *J. Am. Chem. Soc.* **1993**, *115*, 3627.

(17) (a) Medforth, C. J.; Senge, M. O.; Smith, K. M.; Sparks, L. D.; Shelnutt, J. A. *J. Am. Chem. Soc.* **1992**, *114*, 9859. (b) Regev, A.; Galili, T.; Medforth, C. J.; Smith, K. M.; Barkigia, K. M.; Fajer, J.; Levanon, H. *J. Phys. Chem.* **1994**, *98*, 2550. (c) Senge, M. O.; Kalisch, W. W. *Inorg. Chem.* **1997**, *36*, 6103.

(18) Nurco, D. J.; Medforth, C. J.; Forsyth, T. P.; Olmstead, M. M.; Smith, K. M. *J. Am. Chem. Soc.* **1996**, *118*, 10918.

(19) Lin, C. Y.; Hu, S.; Rush, T.; Spiro, T. G. *J. Am. Chem. Soc.* **1996**, *118*, 9452.

(20) Sibilia, S. A.; Hu, S.; Piffat, C.; Melamed, D.; Spiro, T. G. *Inorg. Chem.* **1997**, *36*, 1013.

(21) Takedo, J.; Sato, M. *Chem. Lett.* **1995**, 939.

(22) Kadish, K. M.; D'Souza, F.; Villard, A.; Autret, M.; Van Caemelbecke, E.; Bianco, P.; Antonio, A.; Tagliatesta, P. *Inorg. Chem.* **1994**, *33*, 5169.

(23) D'Souza, F.; Villard, A.; Van Caemelbecke, E.; Franzen, M. M.; Boschi, T.; Tagliatesta, P.; Kadish, K. M. *Inorg. Chem.* **1993**, *32*, 4042.

(24) Kadish, K. M.; Van Caemelbecke, E.; Boulas, P.; D'Souza, F.; Vogel, E.; Kisters, M.; Medforth, C. J.; Smith, K. M. *Inorg. Chem.* **1993**, *32*, 4177.

(25) Bhyrappa, P.; Krishnan, V. *Inorg. Chem.* **1991**, *30*, 239.

(26) DiMagno, S. G.; Williams, R. A.; Therien, M. J. *J. Org. Chem.* **1994**, *59*, 6943.

(27) Kadish, K. M.; Royal, G.; Caemelbecke, E. V.; Gueletti, L. In *The Porphyrin Handbook*; Kadish, K. M., Smith, K. M., Guilard, R., Eds.; Academic Press: New York, 2000; Vol. 9, p 59, and references therein.

(28) Barkigia, K. M.; Berber, M. D.; Fajer, J.; Medforth, C. J.; Renner, M. W.; Smith, K. M. *J. Am. Chem. Soc.* **1990**, *112*, 8851.

(29) Dolphin, D. *J. Heterocycl. Chem.* **1970**, *7*, 275.

(30) Evans, B.; Smith, K. M.; Fuhrhop, J.-H. *Tetrahedron Lett.* **1977**, *5*, 443.

(31) Ono, N.; Muratani, E.; Fumoto, Y.; Ogawa, T.; Tajima, K. *J. Chem. Soc., Perkin Trans. 1* **1998**, 3819.

(32) Wijesekara, T. P.; Matsumoto, A.; Dolphin, D.; Lexa, D. *Angew. Chem., Int. Ed. Engl.* **1990**, *29*, 1028.

(33) (a) Mandon, D.; Ochsenbein, P.; Fischer, J.; Weiss, R.; Jayaraj, K.; Austin, R. N.; Gold, A.; White, P. S.; Brigaud, O.; Battioni, P.; Mansuy, D. *Inorg. Chem.* **1992**, *31*, 2044. (b) Schaefer, W. P.; Hodge, J. A.; Hughes, M. E.; Gray, H. B.; Lyons, J. E.; Ellis, P. E., Jr.; Wagner, R. W. *Acta Crystallogr.* **1993**, *C49*, 1342. (c) Henling, L.; Schaefer, W. P.; Hodge, J. A.; Hughes, M. E.; Gray, H. B. *Acta Crystallogr.* **1993**, *C49*, 1743. (d) Marsh, R. E.; Schaefer, W. P.; Hodge, J. A.; Hughes, M. E.; Gray, H. B. *Acta Crystallogr.* **1993**, *C49*, 1339. (e) Hodge, J. A.; Hill, M. G.; Gray, H. B. *Inorg. Chem.* **1995**, *34*, 809. (f) Birnbaum, E. R.; Hodge, J. A.; Grinstaff, M. W.; Schaefer, W. P.; Henling, L.; Labinger, J. A.; Bercaw, J. E.; Gray, H. B. *Inorg. Chem.* **1995**, *34*, 3625.

(34) DiMagno, S. G.; Williams, R. A.; Therien, M. J. *J. Org. Chem.* **1994**, *59*, 6943.

(35) Chorghade, M. S.; Dolphin, D.; Dupre, D.; Hill, D. R.; Lee, E. C.; Wijesekera, T. P. *Synthesis* **1996**, 1320.

(36) Bhyrappa, P.; Bhavana, P.; Vittal, J. J. *J. Porphyrins Phthalocyanines* **2003**, *7*, 682.

(37) Woller, E. K.; DiMagno, S. G. *J. Org. Chem.* **1997**, *62*, 1588.

(38) (a) Leroy, J.; Bondon, A.; Toupet, L.; Rolando, C. *Chem.−Eur. J.* **1997**, *3*, 1890. (b) Spyroulias, G. A.; Despotopoulos, A. P.; Raptopoulou, A.; Terzis de Montauzon, D.; Poilblanc, R.; Coutsolelos, A. G. *Inorg. Chem.* **2002**, *41*, 2648.

(39) Ono, N.; Kawamura, H.; Maruyama, K. *Bull. Chem. Soc. Jpn.* **1989**, *62*, 3386.

(40) Goll, J. G.; Moore, K. T.; Ghosh, A.; Therien, M. J. *J. Am. Chem. Soc.* **1996**, *118*, 8344.

(41) Ozette, K.; Leduc, P.; Palacio, M.; Bartoli, J.-F.; Barkigia, K. M.; Fajer, J.; Battioni, P.; Mansuay, D. *J. Am. Chem. Soc.* **1997**, *119*, 6442.

(42) Aoyagi, K.; Haga, T.; Toi, H.; Aoyama, Y.; Mizutani, T.; Ogoshi, H. *Bull. Chem. Soc. Jpn.* **1997**, *70*, 937.

(43) Tamaiki, H.; Nagata, Y.; Tsudzuki, S. *Eur. J. Org. Chem.* **1999**, 2471.

(44) Palacio, M.; Mansuy-Mauries, V.; Loire, G.; Le Branch-Ozette, K.; Ledue, P.; Barkigia, K. M.; Fajer, J.; Battioni, P.; Mansuy, D. *Chem. Commun.* **2000**, 1907.

(45) (a) Dolphin, D.; Traylor, T. G.; Xie, L. Y. *Acc. Chem. Res.* **1997**, *30*, 251, and references therein. (b) Ellis, P. E., Jr.; Lyons, J. E. *Coord. Chem. Rev.* **1990**, *105*, 181. (c) Hoffmann, P.; Labat, G.; Robert, A.; Meunier, B. *Tetrahedron Lett.* **1990**, *31*, 1991. (d) Lyons, J. E.; Ellis, P. E. *Catal. Lett.* **1991**, *8*, 45.

(46) Sheldon, R. A. *Metalloporphyrins in Catalytic Oxidations*; Marcel Dekker: New York, 1994.

(47) Montanari, F.; Casella, L. *Metalloporphyrins in Catalysed Oxidations*; Kluwer Academic Publishers: Dordrecht, The Netherlands, 1994.

(48) Grinstaff, M. W.; Hill, M. G.; Labinger, L. A.; Gray, H. B. *Science* **1994**, *264*, 1311.

(49) Meunier, B. *Chem. Rev.* **1992**, *92*, 1411.

(50) Ellis, P. E., Jr.; Lyons, J. E. *Coord. Chem. Rev.* **1990**, *105*, 181.

(51) Traylor, T. G.; Tsuchiya, S. *Inorg. Chem.* **1987**, *26*, 1338.

(52) Takeuchi, T.; Gray, H. B.; Goddard, W. A., III. *J. Am. Chem. Soc.* **1994**, *116*, 9730.

(53) D'Souza, F.; Zandler, M.; Tagliatesta, P.; Ou, Z.; Shao, J.; Van Caemelbecke, E.; Kadish, K. M. *Inorg. Chem.* **1998**, *37*, 4567.

(54) Takeda, J.; Sato, M. *Chem. Lett.* **1995**, 971.

(55) (a) Bhyrappa, P.; Bhavana, P. *Chem. Phys. Lett.* **2001**, *342*, 39. (b) Bhyrappa, P.; Arunkumar, C.; Varghese, B. *J. Porphyrins Phthalocyanines* **2007**, *11*, 795.
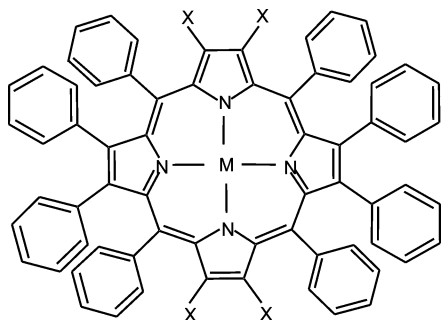
M = 2H, X = CN , Cl, Br
M = Ni(II), X = CN
M = Zn(II), X = Cl

Figure 1. Chemical structures of mixed substituted porphyrins and their metal complexes.

groups.[59−62] The mixed substituted porphyrins exhibited an interesting trend in their electronic spectral and electrochemical redox properties.[62] The pronounced changes in properties of the β-pyrrole substituted porphyrins in contrast to *meso*-phenyl functionalized porphyrins were due to the substituents which are in direct conjugation with the extended π system. The introduction of antipodal tetrasubstitution as in $H_2(TPPR_4)$ (R = C_6H_5, CH_3, Br)[63] exhibited a nearly planar porphyrin ring, while the corresponding five-coordinated Zn(II) complexes[64] showed moderate nonplanar geometry. Crystal structures of $M(TPPR_8)$'s bearing similar electron-donor (R = alkyl or aryl groups)[3,8,16,17,28] and electron-withdrawing[33,36,38] substituents feature nonplanar distortion of the macrocyclic ring, and it varies with the size of the β-pyrrole substituents.[1] The role of mixed β-pyrrole sub-stituents on the porphyrin macrocyclic ring conformations has been largely unexamined.[59,60,62] In the present work, the crystal structures of a series of free base derivatives ($H_2(TPP(Ph)_4X_4)$; X = CN, Cl, Br) with varying steric crowding at the periphery of the porphyrin have been elucidated (Figure 1). These free base porphyrin derivatives and their metal complexes feature dramatic differences in their stereochemistry in contrast to the porphyrins bearing similar β-pyrrole substituents.

Experimental Section

Materials. 2,3,5,10,12,13,15,20-Octaphenylporphyrin, $H_2(TPP(Ph)_4)$, was prepared using the reported procedure.[63d] 2,3,12,13-Tetrabromo-5,7,8,10,15,17,18,20-octaphenylporphyrin ($H_2(TPP(Ph)_4$-

$Br_4)$), 2,3,12,13-tetrachloro-5,7,8,10,15,17,18,20-octaphenylporphyrin ($H_2(TPP(Ph)_4Cl_4)$), 2,3,12,13-tetracyano-5,7,8,10,15,17,18,20-octaphenylporphyrin ($H_2(TPP(Ph)_4(CN)_4)$), 2,3,12,13-tetracyano-5,7,8,10,15,17,18,20-octaphenylporphinato nickel(II) ($Ni(TPP(Ph)_4(CN)_4)$), and 2,3,12,13-tetrachloro-5,7,8,10,15,17,18,20-octaphenylporphinato zinc(II) ($Zn(TPP(Ph)_4Cl_4)$) complexes were synthesized using slightly modified literature methods.[62] All of the solvents employed in this study were of analytical reagent grade and distilled prior to use.[65]

The mixed substituted free base porphyrins and their metal complexes were characterized by electronic absorption and ^{1}H NMR and mass spectroscopic methods. **$H_2(TPP(Ph)_4(CN)_4)$.** Electronic absorption spectrum in CH_2Cl_2, λ_{max}, nm (log ε): 465 (5.16), 584 (3.96), 621 (3.98), 779 (4.15). ^{1}H NMR in $CDCl_3$: 7.85 (d, 8H, *meso-o*-phenyl-H), 7.50 (t, 4H, *meso-p*-phenyl-H), 7.40 (t, 8H, *meso-m*-phenyl-H), 6.84 (m, 20H, β-pyrrole-phenyl-H), −1.48 (s, 2H, imino-H). ESI-MS (*m/z*): 1019.22 (calcd, 1019.18). **$H_2(TPP$-$(Ph)_4Cl_4)$.** λ_{max}, nm (log ε): 375 (4.36), 464 (5.20), 568 (3.92), 621 (3.96), 718 (4.05). ^{1}H NMR in $CDCl_3$: 7.95 (d, 8H, *meso-o*-phenyl-H), 7.30 (m, 12H, *meso-m* and *p*-phenyl-H), 6.85 (m, 20H, β-pyrrole-phenyl-H), −1.80 (bs, 2H, imino-H). ESI-MS (*m/z*): 1057 (calcd, 1056.92). **$H_2(TPP(Ph)_4Br_4)$.** λ_{max}, nm (log ε): 378 (4.32), 469 (5.16), 574 (3.94), 630 (3.94), 734 (3.97). ^{1}H NMR in $CDCl_3$: 7.85 (d, 8H, *meso-o*-phenyl-H), 7.23 (m, 12H, *meso-m*- and *p*-phenyl-H), 6.75 (m, 20H, β-pyrrole-phenyl-H), −1.79 (bs, 2H, imino-H). ESI-MS (*m/z*): 1235 (calcd, 1234.72). **$Zn(TPP(Ph)_4Cl_4)$.** λ_{max}, nm (log ε): 365 (4.42), 455 (5.26), 587 (4.10), 636 (3.95). ^{1}H NMR in $CDCl_3$: 7.66 (d, 8H, *meso-o*-phenyl-H), 7.16 (m, 12H, *meso-m*- and *p*-phenyl-H), 6.70 (m, 20H, β-pyrrole phenyl-H). MALDI-TOF-MS (*m/z*): 1120.10 (calcd, 1120.28). **$Ni(TPP(Ph)_4(CN)_4)$.** λ_{max}, nm (log ε): 344 (4.34), 457 (5.10), 546 (3.81), 590 (sh), 653 (4.45). ^{1}H NMR in $CDCl_3$: 7.36 (d, 8H, *meso-o*-phenyl-H), 7.31 (t, 4H, *meso-p*-phenyl-H), 7.09 (t, 8H, *meso-m*-phenyl-H), 6.89 (t, 4H, β-pyrrole-*p*-phenyl-H), 6.80 (t, 8H, β-pyrrole-*m*-phenyl-H), 6.71 (d, 8H, β-pyrrole-*o*-phenyl-H). MALDI-TOF-MS (*m/z*): 1075.18 (calcd, 1075.85).

Crystal Structures. Single-crystal X-ray structure data collections were performed on a Bruker AXS Kappa Apex II CCD diffractometer with graphite monochromated Mo Kα radiation (λ = 0.71073 Å). The crystals were coated with inert oil, mounted on a glass capillary, and transferred to the cold nitrogen gas stream of the diffractometer, and crystal data were collected at 173 K. The reflections with $I > 2\sigma(I)$ were employed for structure solution and refinement. The SIR92[66a] (WINGX32) program was used for solving the structure by direct methods. Successive Fourier synthesis was employed to complete the structures after full-matrix least-squares refinement on $|F|^2$ using the SHELXL97[66b] software. Fourier syntheses led to the location of all of the non-hydrogen atoms. For the structure refinement, all data were used including negative intensities. The criterion of $F^2 > 2\sigma(F^2)$ was employed for calculating R_1. R factors based on F^2 (wR_2) are statistically about twice as large as those based on F, and R factors based on all data will be even larger. Non-hydrogen atoms were refined with anisotropic thermal parameters. All of the hydrogen atoms in the porphyrin structure could be located in the difference map. However, the hydrogen atoms were geometrically relocated at chemically meaningful positions and were given riding model refinement.

(56) Takeda, J.; Ohya, T.; Sato, M. *Inorg. Chem.* **1992**, *31*, 2877.
(57) (a) Bhyrappa, P.; Krishnan, V.; Nethaji, M. *Chem. Lett.* **1993**, 869. (b) Tabata, M.; Nishimoto, J.; Ogata, A.; Kusano, T.; Nahar, N. *Bull. Chem. Soc. Jpn.* **1996**, *69*, 673.
(58) Sutter, T. P. G.; Hambright, P. *J. Coord. Chem.* **1993**, *30*, 317.
(59) Senge, M. O.; Gerstung, V.; Ruhlandt-Senge, K.; Runge, S.; Lehmann, I. *J. Chem. Soc., Dalton Trans.* **1998**, 4187.
(60) Duval, H.; Bulach, V.; Fischer, J.; Weiss, R. *Inorg. Chem.* **1999**, *38*, 5495.
(61) Leroy, J.; Porhiel, E.; Bondon, A. *Tetrahedron* **2002**, *58*, 6713.
(62) Bhyrappa, P.; Sanker, M.; Varghese, B. *Inorg. Chem.* **2006**, *45*, 4136.
(63) (a) Chan, K. S.; Zhou, X.; Lou, B.-S.; Mak, T. C. W. *J. Chem. Soc., Chem. Commun.* **1994**, 271. (b) Bhyrappa, P.; Karunanithi, K.; Varghese, B. *Acta Crystallogr.* **2008**, *E64*, m330. (c) Zou, J.-H.; Xu, Z. I. M.; You, X.-Z. *Acta Crystallogr.* **1995**, *C51*, 760. (d) Bhyrappa, P.; Karunanithi, K.; Varghese, B. *Acta Crystallogr.* **2007**, *E63*, o4755.
(64) Terazono, Y.; Patrick, B. O.; Dolphin, D. *Inorg. Chem.* **2002**, *41*, 6703.
(65) Armarego, W. L. F.; Chai, C. L. L. *Purification of Laboratory Chemicals*; Elsevier: New York, 2003.
(66) (a) Altomare, A. G.; Cascarano, G.; Giacovazzo, C.; Gualardi, A. *J. Appl. Crystallogr.* **1993**, *26*, 343. (b) Sheldrick, G. M. *SHELXL97*; University of Göettingen: Göettingen, Germany, 1997. (c) Spek, A. L. *J. Appl. Crystallogr.* **2003**, *36*, 7.

Table 1. Crystal Structure Data of Mixed Substituted Porphyrins and Their Metal Complexes, **1**, $H_2(TPP(Ph)_4(CN)_4) \cdot 3(C_2H_4Cl_2)$; **2**, $H_2(TPP(Ph)_4Cl_4) \cdot 2(CH_3OH)$; **3**, $H_2(TPP(Ph)_4Br_4) \cdot 2THF \cdot 1.5(CH_3OH)$; **4**, $Ni(TPP(Ph)_4(CN)_4) \cdot C_6H_{14} \cdot 0.5(C_2H_4Cl_2)$; and **5**, $Zn(TPP(Ph)_4Cl_4)(Py) \cdot C_2H_4Cl_2$

	1	**2**	**3**	**4**	**5**
empirical formula	$C_{78}H_{54}Cl_6N_8$	$C_{70}H_{50}Cl_4N_4O_2$	$C_{77.5}H_{62}Br_4N_4O_{3.5}$	$C_{79}H_{56}ClN_8Ni$	$C_{75}H_{49}Cl_6N_5Zn$
fw	1315.99	1120.94	1426.96	1211.48	1298.26
color	green	green	black	brown	purple
cryst syst	monoclinic	monoclinic	triclinic	triclinic	monoclinic
space group	$P2_1/n$	$P2_1/c$	$P\bar{1}$	$P\bar{1}$	$P2_1/n$
a, Å	17.9279(5)	15.8098(6)	13.1059(3)	14.1775(7)	13.6590(3)
b, Å	19.9174(6)	27.6166(8)	16.1824(3)	15.6420(7)	12.4972(3)
c, Å	19.7750(6)	13.7545(4)	17.7714(4)	16.0408(8)	36.3352(9)
α, (deg)			113.3310(10)	65.001(2)	
β, (deg)	109.800(10)	102.6770(10)	94.8680(10)	82.372(2)	90.5380(10)
γ, (deg)			107.2520(10)	74.191(2)	
vol (Å³)	6643.7(3)	5859.0(3)	3215.98(12)	3101.4(3)	6202.1(3)
Z	4	4	2	2	4
D_{calcd} (mg/m³)	1.316	1.271	1.474	1.297	1.390
wavelength (λ), Å	0.71073	0.71073	0.71073	0.71073	0.71073
T (K)	173(2)	173(2)	173(2)	173(2)	173(2)
no. of unique reflections	11691	10308	11177	10836	10908
no. of params refined	831	738	771	783	766
GOF on F^2	1.049	1.032	1.065	1.048	1.029
$R_1{}^a$	0.0855	0.0666	0.0644	0.0763	0.0702
$wR_2{}^b$	0.2242	0.1742	0.1776	0.2289	0.1806

$^a R_1 = \sum||F_o| - |F_c||/\sum|F_o|$; $I_o > 2\sigma (I_o)$. $^b wR_2 = [\sum w(F_o^2 - F_c^2)^2/\sum w(F_o^2)^2]^{1/2}$.

Crystals of the free base porphyrins and their metal complexes were grown at room temperature. $H_2(TPP(Ph)_4(CN)_4) \cdot 3(C_2H_4Cl_2)$ was crystallized from the vapor diffusion of methanol to a 1,2-dichloroethane solution of the porphyrin over a period of seven days. All three lattice solvates showed positional disorder and were refined with the sum of their individual occupancies equal to 1.0. Crystals of $H_2(TPP(Ph)_4Cl_4) \cdot 2(CH_3OH)$ were obtained by the vapor diffusion of methanol to the porphyrin in 1,2-dichloroethane over a duration of five days. $H_2(TPP(Ph)_4Br_4) \cdot 2(THF) \cdot 1.5(CH_3OH)$ crystals were grown by the diffusion of methanol vapor to the porphyrin in THF over a period of five days. This structure shows positional disorder of one of the THF and methanol solvates. The hydrogen atoms of these solvates were not observed in the difference map and could not be fixed reliably. $Ni(TPP(Ph)_4(CN)_4) \cdot (C_6H_{14}) \cdot 0.5(C_2H_4Cl_2)$ crystals were obtained by the vapor diffusion of hexane to the porphyrin in 1,2-dichloroethane for a period of four days. The hexane solvate showed positional disorder. Hydrogen atoms of the hexane solvate were not observed in the difference map. The structure was refined without fixing the hydrogen atoms for hexane solvate. $Zn(TPP(Ph)_4Cl_4)(Py) \cdot (C_2H_4Cl_2)$ was crystallized by the vapor diffusion of hexane to the 1,2-dichloroethane solution of the Zn(II) porphyrin containing few drops of pyridine for a duration of six days. The axial pyridine, one of the β-pyrrole phenyls, and the lattice 1,2-dichloroethane showed positional disorder. The intermolecular contacts were calculated using the Platon[66c] program.

Results and Discussion

Crystal structures of numerous highly substituted porphyrins have been reported in the literature,[1] and the different structural distortion of the macrocyclic ring was examined by Scheidt and Lee.[67,68] The nonplanar conformation of the porphyrins may be altered by varying the size and number of the peripheral substituents.[1,2] The $H_2(TPP(Ph)_4X_4)$ derivatives and their metal [$Ni(TPP(Ph)_4(CN)_4)$ and Zn(TPP-

$(Ph)_4Cl_4$)] complexes were synthesized and characterized by electronic absorption and ^1H NMR and mass spectroscopic methods. The stereochemistry of the macrocycle in $H_2(TPP(Ph)_4X_4)$ (X = CN, Cl, Br) was examined by varying the β-pyrrole substituents X at the antipodal positions. Table 1 lists the crystal structure data of the solvated structures of mixed substituted free base tetraphenylporphyrins and their metal complexes. To compare the extent of steric crowding induced by the substituent (X) and phenyl groups at the antipodal β-pyrrole positions, the selected mean bond lengths and geometrical parameters of the porphyrin skeleton are compared for the solvated $H_2(TPP(Ph)_4X_4)$ structures and are listed in Table 2. A comparison is made with the symmetrically substituted 2,3,5,7,8,10,12,13,15,17,18,20-dodecaphenylporphyrin trihydrate, $H_2(DPP) \cdot 3(H_2O)$, structure[69] to elucidate the influence of mixed substitution on the stereochemistry of the macrocyclic ring.

The ORTEP diagrams of the porphyrin ring of the solvated $H_2(TPP(Ph)_4X_4)$ (X = CN, Cl, Br) structures along with the atomic numbering scheme are shown in Figure 2. These porphyrins feature bond lengths of the 24-atom core that are comparable to the reported saddle-shaped $H_2(DPP) \cdot 3(H_2O)$ structure[17] and other similarly solvated $H_2(DPP)$ structures,[17b,70] but they showed interesting differences in their geometrical parameters. The presence of differing sizes and shapes of the substituents (X) in the mixed substituted porphyrins, $H_2(TPP(Ph)_4X_4)$, is anticipated to generate variation in steric crowding at the periphery of the macrocycle. The parent 2,3,5,10,12,13,15,20-octaphenylporphyrin showed almost planar geometry of the porphyrin ring.[63a] As suggested previously,[68] the elongation of the core (N_4H_2) is due to the steric strain enforced by the peripheral groups, and this results from the bulky C_b,C_b substituents that push the adjacent *meso*-phenyl groups toward other pyrroles with less
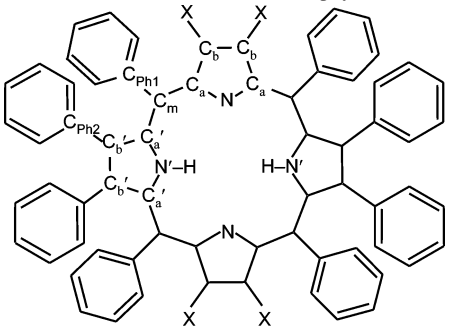
(67) Scheidt, W. R.; Lee, Y. J. *Struct. Bonding (Berlin)* **1987**, *64*, 1.
(68) Scheidt, W. R. In *The Porphyrin Handbook*; Kadish, K. M., Smith, K. M., Guilard, R., Eds.; Academic Press: New York, 2000; Vol. 3, p 49.
(69) Barkigia, K. M.; Nurco, D. J.; Renner, M. W.; Melamed, D.; Smith, K. M.; Fajer, J. *J. Phys. Chem. B* **1998**, *102*, 322.
(70) Senge, M. O. *Z. Naturforsch.* **1999**, *54b*, 662.

Table 2. Comparison of Selected Mean Bond Lengths and Geometrical Parameters of Free-Base Mixed Substituted Porphyrins

X = CN, $H_2(TPP(Ph)_4(CN)_4) \cdot 3(C_2H_4Cl_2)$, **1**

X = Cl, $H_2(TPP(Ph)_4Cl_4) \cdot 2(CH_3OH)$, **2**

X = Br, $H_2(TPP(Ph)_4Br_4) \cdot 2(THF) \cdot 1.5(CH_3OH)$, **3**

X = Ph, $H_2(DPP) \cdot 3(H_2O)$

	1	**2**	**3**	$H_2(DPP) \cdot 3(H_2O)^a$
		Bond Lengths (Å)		
C_a-N	1.361(5)	1.360(4)	1.362(6)	1.357(4)
$C_a'-N'$	1.373(5)	1.379(4)	1.359(5)	
C_a-C_b	1.450(5)	1.459(5)	1.445(7)	1.442(2)
$C_a'-C_b'$	1.444(5)	1.437(5)	1.443(7)	
C_b-C_b	1.378(5)	1.345(5)	1.351(8)	1.370(2)
$C_b'-C_b'$	1.380(5)	1.380(5)	1.381(7)	
C_a-C_m	1.415(6)	1.409(5)	1.413(7)	1.410(2)
$C_a'-C_m$	1.398(5)	1.412(5)	1.415(7)	
		Bond Angles (deg)		
C_a-N-C_a	107.2(3)	107.8(3)	108.2(4)	109.4(14)
$C_a'-N'-C_a'$	111.0(3)	110.4(3)	110.9(4)	
$C_a-C_m-C_a'$	124.0(3)	122.3(3)	121.3(4)	122.1(11)
$N-C_a-C_m$	126.0(3)	122.7(3)	122.6(4)	123.0(11)
$N'-C_a'-C_m$	124.3(3)	125.3(3)	123.5(5)	
$N-C_a-C_b$	110.0(3)	109.1(3)	108.7(4)	107.9(10)
$N'-C_a'-C_b'$	106.6(3)	106.7(3)	107.2(4)	
$C_a-C_b-C_b$	106.4(3)	107.0(3)	107.2(4)	107.1(10)
$C_a'-C_b'-C_b'$	107.8(3)	107.9(3)	107.3(4)	
$C_b-C_a-C_m$	124.0(3)	128.2(3)	128.7(5)	129.0(11)
$C_b'-C_a'-C_m$	128.9(3)	127.9(3)	129.2(5)	
$C_a-C_m-C_{ph1}$	116.8(3)	120.1(3)	119.9(4)	118.9(11)
$C_a'-C_m-C_{ph1}$	119.1(3)	117.7(3)	118.8(4)	
C_a-C_b-X	130.5(4)	128.1(3)	127.8(4)	126.1(11)
$C_a'-C_b'-C_{ph2}$	127.7(3)	125.3(3)	125.1(4)	
		Distance (Å)		
$N \cdots N$	4.044(3)	4.245(4)	4.230(4)	4.291
$N' \cdots N'$	4.227(3)	4.122(4)	4.182(6)	4.235
		Average Dihedral Angle Relative to Mean Plane (deg)		
meso-phenyl	51.7(3)	41.7(2)	26.4(3)	n.a.
β-phenyl	64.1(2)	54.8(2)	51.3(3)	n.a.
pyrrole (X)	25.5(2)	29.3(6)	39.8(2)	n.a.
pyrrole (Ph)	18.7(1)	35.9(1)	36.7(2)	n.a.

^{a} Data are from ref 69; n.a., data not available.

sterically crowded C_b',C_b' positions. The relief of steric strain results in $C_b-C_b > C_b'-C_b'$ and $C_a-C_m-C_{ph1} > C_a'-C_m-C_{ph1}$ parameters. Surprisingly, solvated $H_2(TPP(Ph)_4-X_4)$ (X = Br, Cl) structures showed $C_b-C_b < C_b'-C_b'$ and $C_a-C_m-C_{ph1} > C_a'-C_m-C_{ph1}$. This is perhaps due to the influence of steric and electronic factors.[68] However, the $H_2(TPP(Ph)_4(CN)_4) \cdot 3(C_2H_4Cl_2)$ structure exhibited almost similar C_b-C_b and $C_b'-C_b'$ bond distances with lowered $C_a-C_m-C_{ph1}$ relative to $C_a'-C_m-C_{ph1}$ angles. Furthermore, the smaller X group at the pyrrole position moves away from the adjacent *meso*-phenyl groups, resulting in an increased C_a-C_b-X angle and decrease in the $C_a'-C_b'-C_{ph2}$ angle. For solvated $H_2(TPP(Ph)_4X_4)$ structures, the $C_a-C_b-X >$
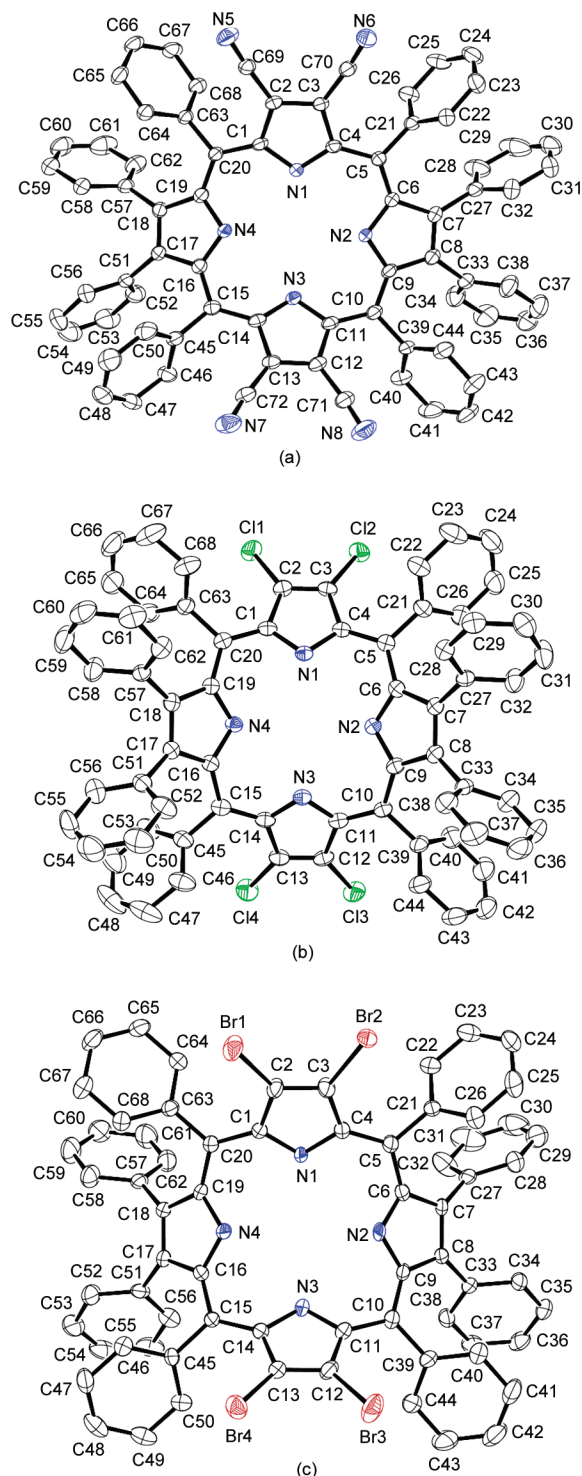
Figure 2. ORTEP diagrams of (a) $H_2(TPP(Ph)_4(CN)_4) \cdot 3(C_2H_4Cl_2)$, (b) $H_2(TPP(Ph)_4Cl_4) \cdot 2(CH_3OH)$, and (c) $H_2(TPP(Ph)_4Br_4) \cdot 2THF \cdot 1.5(CH_3OH)$. Solvate and hydrogens are not shown for clarity. Thermal ellipsoids shown at 40% probability level.

$C_a'-C_b'-C_{ph2}$ angle follows the order CN > Cl > Br, and the change in the angle is $2-3°$ (Table 2).

A previous report on the antipodal β-tetrasubstituted $H_2(TPPBr_4)$ structure[63c] showed that the C_b-C_b bond distance of the pyrroles with Br groups is shorter (1.33(2) Å), while the other unsubstituted pyrroles feature longer $C_b'-C_b'$ bond distances (1.36(2) Å). An opposite trend ($C_b-C_b > C_b'-C_b'$) was reported in the case of $H_2(TPPR_4)$

(R = CH$_3$, C$_6$H$_5$) structures.[63a,b] Further, the hydrogens located on the transannular pyrrole nitrogens bearing β-phenyls showed a greater C$_a$'−N'−C$_a$' angle relative to the C$_a$−N−C$_a$ angle by 2−4° along the other transannular pyrroles with X substituents. The relief of steric strain also results in C$_b$−C$_a$−C$_m$ < C$_b$'−C$_a$'−C$_m$ angles for smaller substituents (X) along the transannular β-pyrrole direction. Such a trend in angles is observed for the H$_2$(TPP(Ph)$_4$(CN)$_4$)·3(C$_2$H$_4$Cl$_2$) structure, while they are approximately similar in the solvated H$_2$(TPP(Ph)$_4$X$_4$) (X = Cl, Br) structures. This suggests that the antipodal halogen substituents induce greater steric crowding than the smaller cyano groups with respect to β-phenyl groups. The separation between the transannular nitrogens is found to be N···N > N'···N' in solvated H$_2$(TPP(Ph)$_4$X$_4$) (X = Cl, Br) structures, but an opposite trend is observed in the H$_2$(TPP(Ph)$_4$(CN)$_4$)·3(C$_2$H$_4$Cl$_2$) structure (Table 2). This also indicates that the elongation of the core is more along the transannular pyrroles with halogens as in the former structures, and it is along the other pyrroles with phenyl groups in the latter structure. Nevertheless, in all three mixed substituted free base porphyrins, the average size of the N$_4$H$_2$ core decreased when compared to the H$_2$DPP·3(H$_2$O) structure and varies in the order H$_2$(TPP(Ph)$_4$(CN)$_4$) < H$_2$(TPP(Ph)$_4$Cl$_4$) < H$_2$(TPP(Ph)$_4$Br$_4$). In these solvated H$_2$(TPP(Ph)$_4$X$_4$) (X = CN, Cl, Br) structures, the C$_a$−C$_m$ (mean value of C$_a$−C$_m$ and C$_a$'−C$_m$) bond distance increases as anticipated; however, the C$_a$−C$_m$−C$_a$' angle decreases with the increase in core size (Table 2). It is known that, as the core size increases, the meso bridges open up, resulting in an increase in the C$_a$−C$_m$ bond length and C$_a$−C$_m$−C$_a$' angle.[3,28] This is probably due to the relaxation in steric strain induced by the differing shapes and sizes of the antipodal mixed substituents. It is worthy to note that the H$_2$(TPP(Ph)$_4$Br$_4$) showed nonplanarity of the ring similar to that reported for H$_2$(DPP)·3(H$_2$O) and H$_2$(TPPBr$_8$)·DMF[38b] structures. Moderately sterically crowded β-tetrasubstituted porphyrins, H$_2$(TPPX$_4$) (X = C$_6$H$_5$, CH$_3$, Br), exhibited a nearly planar macrocyclic ring with the elongation of the core (N···N) along the substituted β-pyrrole direction.[63] The short intramolecular contact distance between C$_{ph1}$ and C$_{CN}$ was found to be 2.850(4) Å, and the (C$_\beta$−C≡N)$_{av}$ angle is 174.3(2)°, indicating the extent of steric crowding between the meso-phenyl and the β-pyrrole CN groups. Similarly, the close contact in C$_{ph1}$···X (X = Cl, Br) was found to be 3.155(4) and 3.224(3) Å in solvated H$_2$(TPP(Ph)$_4$Cl$_4$) and H$_2$(TPP(Ph)$_4$Br$_4$) structures, respectively. The intermolecular short contact between the β-pyrrole (CN)N, Cl, and Br groups and the adjacent meso-o-phenyl carbon is 3.38(5), 3.16(4), and 3.23(4) Å, respectively, for the corresponding H$_2$(TPP(Ph)$_4$X$_4$) (X = CN, Cl, Br) structures.

The edge-on views of the free base porphyrin structures along the transannular direction (N1···N3) are shown in Figure 3. These structures showed enhanced distortion of the macrocyclic ring from planarity. The mean plane displacement of the core atoms from the porphyrin ring plane (Figure 4) shows that the pyrrole rings are displaced alternatively up and down from the 24-atom core with minimal displacement of the meso-carbons. However, H$_2$(TPP(Ph)$_4$(CN)$_4$)·3C$_2$H$_4$Cl$_2$ shows considerable displace-

(a)

(b)

(c)
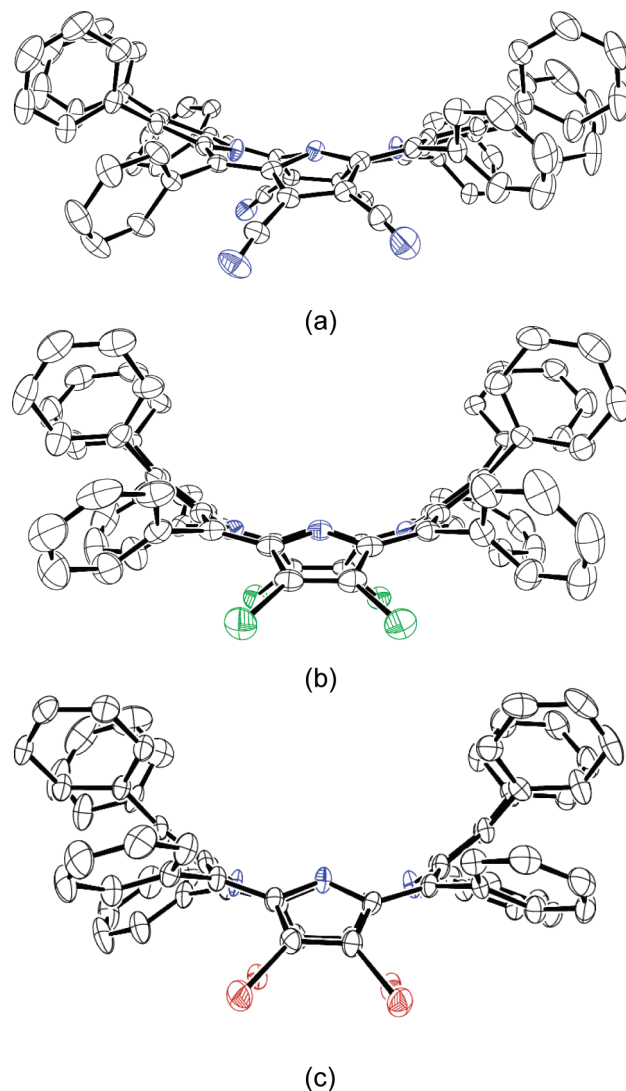
Figure 3. ORTEP diagrams showing the edge-on view of (a) H$_2$(TPP-(Ph)$_4$(CN)$_4$)·3(C$_2$H$_4$Cl$_2$), (b) H$_2$(TPP(Ph)$_4$Cl$_4$)·2(CH$_3$OH), and (c) H$_2$(TPP-(Ph)$_4$Br$_4$)·2THF·1.5(CH$_3$OH) structures. Hydrogen atoms and lattice solvates are not shown for clarity. Thermal ellipsoids shown at the 40% probability level.

ment of the meso-carbon and β-pyrrole carbons (Figure 4a). The linear display of the core atoms indicates that the H$_2$(TPP(Ph)$_4$(CN)$_4$)·3(C$_2$H$_4$Cl$_2$) has a less nonplanar conformation when compared to solvated H$_2$(TPP(Ph)$_4$X$_4$) (X = Cl, Br) structures (Figure 4b,c). The displacement of pyrrole carbons and the meso-carbons indicates that these free base structures exhibit more of saddle distortion combined with a varying degree of ruffled and domed conformations.[67,68] In the case of H$_2$(TPP-(Ph)$_4$(CN)$_4$)·3(C$_2$H$_4$Cl$_2$), the average deviation of the cyano carbon (C69, C70, C71, and C72) atoms is +0.072(3) Å, while the phenyl carbons (C27, C33, C51, and C57) attached to the β-pyrrole carbon (C$_b$) exhibit an opposite deviation from their corresponding mean plane of the pyrrole ring by −0.030(3) Å. The adjacent halo groups tilt from each other within 0.011(3) Å in H$_2$(TPP(Ph)$_4$X$_4$) (X = Cl, Br) structures with approximately similar deviation in the phenyl carbon (C$_{ph2}$) attached to the β-pyrrole positions. In the H$_2$(TPP-(Ph)$_4$X$_4$) structures, the phenyl rings are oriented perpendicular to the

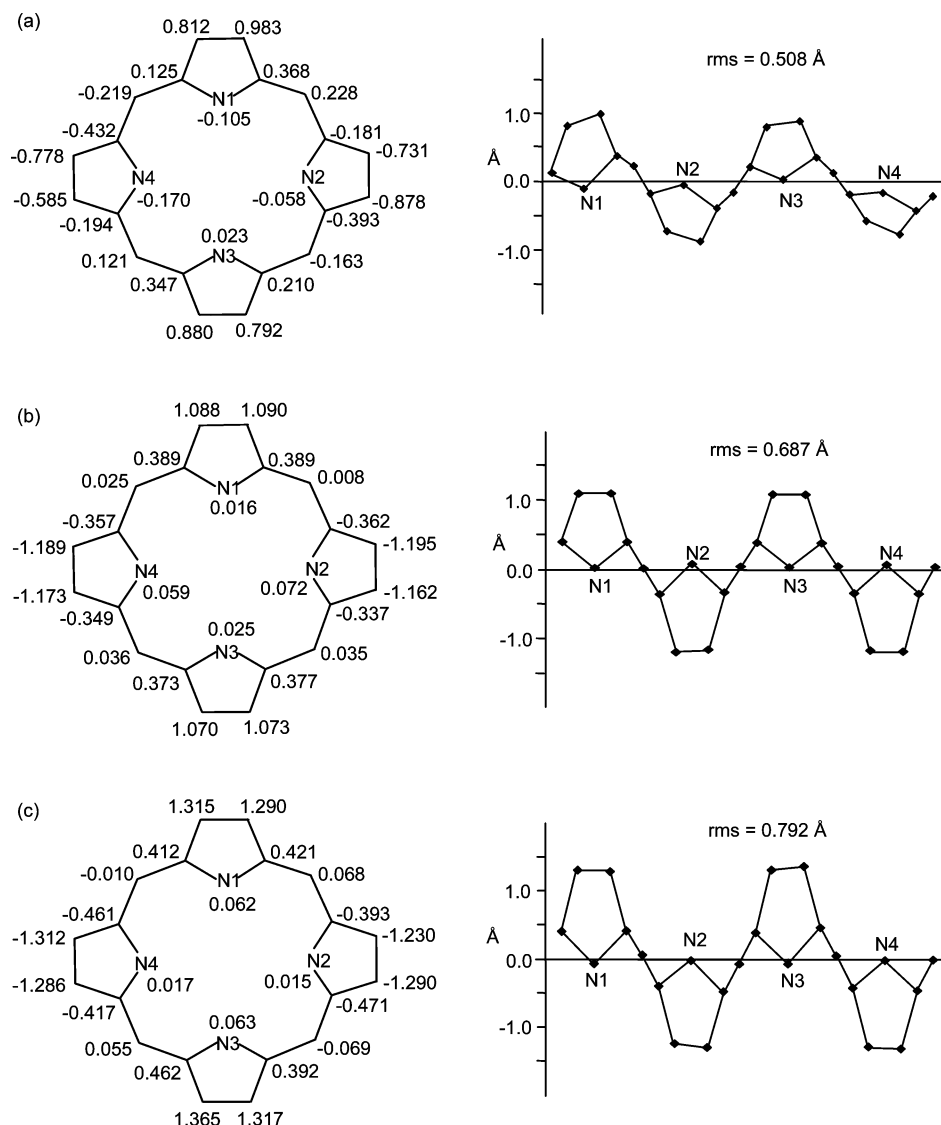**Figure 4.** (left column) Mean plane displacements (in ångstroms, esd's 0.004 Å) of the 24-atom core. (right column) Linear display (in ångstroms) of the skeletal atoms for (a) $H_2(TPP(Ph)_4(CN)_4) \cdot 3(C_2H_4Cl_2)$, (b) $H_2(TPP(Ph)_4Cl_4) \cdot 2(CH_3OH)$, and (c) $H_2(TPP(Ph)_4Br_4) \cdot 2THF \cdot 1.5(CH_3OH)$ structures.

24-atom core with C_m-C_{ph1} and C_b-C_{Ph2} bond lengths that are in the range 1.480−1.495 Å, indicating very minimal conjugation between the phenyl groups with the porphyrin π system. The extent of steric crowding at the periphery of the porphyrin is anticipated to be in the same order as the van der Waals radii of the X groups, and it follows the order Br > Cl > (C) CN.[71] The extent of distortion of the macrocycle in $H_2(TPP(Ph)_4X_4)$ (X = CN, Cl) structures is significantly less relative to $H_2(DPP) \cdot 3(H_2O)$, and it is comparable to that of $H_2(TPP(Ph)_4Br_4) \cdot 2(THF) \cdot 1.5(CH_3OH)$ (Table 2, Figure 4).

As observed, the steric crowding varies with the size of the X groups in $H_2(TPP(Ph)_4X_4)$ (X = CN, Cl, Br) structures. To avoid steric repulsion among the peripheral substituents, pyrrole rings tilt and phenyl groups twist from the mean plane of the porphyrin ring. *meso*- and β-Pyrrole phenyl groups are nearly planar (within 0.01 Å), oriented perpendicular to the porphyrin ring, and the degree of twist of these groups showed severe dependence on the nonplanarity of the macrocyclic ring (Table 2). The average dihedral angle of the *meso*-phenyl groups is lower in contrast to the β-pyrrole

phenyl groups, and it increases with a decrease in nonplanarity and follows the order $H_2(TPP(Ph)_4Br_4)$ < $H_2(TPP(Ph)_4Cl_4)$ < $H_2(TPP(Ph)_4(CN)_4)$. The root-mean-square displacement of the core atoms also suggests that the extent of nonplanarity follows the size of the X groups (Figure 4). The free base porphyrin structures feature intramolecular hydrogen-bonding interactions within the N_4H_2 core. Similar bifurcated hydrogen bonding was observed in $H_2(TPPBr_8) \cdot 2(DMF)^{38b}$ and $H_2(DPP) \cdot 3(H_2O)^{69}$ structures. It can be seen that the average nitrile (C≡N) bond length in $H_2(TPP(Ph)_4-(CN)_4) \cdot 3(C_2H_4Cl_2)$ is found to be longer (1.146(6) Å) and the β-pyrrole (C) to the cyano carbon shorter (1.427(6) Å) when compared to the corresponding distances known for the dodeca-substituted $Ni(TPP(CN)_4Br_4) \cdot 2.5(C_2H_4Cl_2)$ complex [1.064(15), 1.458(18) Å].[62] The center-to-center distance between the adjacent phenyl rings in all of these structures was in the range of 3.45−4.61 Å.

The crystal structures were examined for any intermolecular contacts which could be responsible for the nonplanar

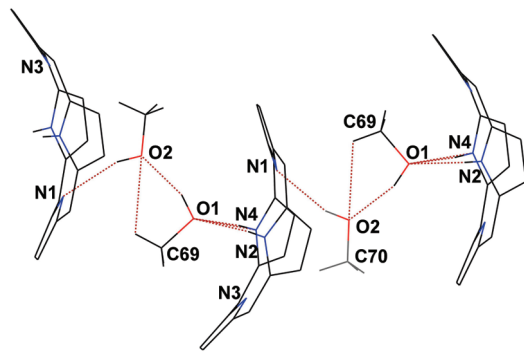(71) Bondi, A. *J. Phys. Chem.* **1964**, *68*, 441.

Figure 5. The hydrogen-bonding interactions of the $H_2(TPP(Ph)_4Cl_4) \cdot 2(CH_3OH)$ structure via $CH_3OH \cdots HOCH_3$ ($O1 \cdots O2$) and porphyrin $\cdots HOCH_3$ ($N \cdots O$) along the unit cell c axis. Hydrogen-bonding interactions are shown in dotted pink lines. The phenyl and chloride groups are omitted for clarity.

conformations in these mixed substituted free base porphyrins. In the case of the $H_2(TPP(Ph)_4(CN)_4) \cdot 3C_2H_4Cl_2$ structure, a close contact distance of $C73 \cdots N3 = 3.308(13)$ Å ($C-H \cdots N$) is observed for porphyrin $\cdots C_2H_4Cl_2$ interactions. For the $H_2(TPP(Ph)_4Br_4) \cdot 2THF \cdot 1.5(CH_3OH)$ structure, the closest hydrogen-bonding intermolecular distance ($N-H \cdots O$) $N2 \cdots O1 = 3.00(4)$ Å is found to be between the core and the disordered THF solvate. A very short $N3 \cdots O2 = 2.79(3)$ Å was also observed between the core with the disordered methanol solvate. The $H_2(TPP(Ph)_4Cl_4) \cdot 2(CH_3OH)$ structure shows interesting solvate-induced intermolecular hydrogen-bonding interactions. The hydrogen-bonding interactions of the porphyrin core $\cdots$ methanol and $CH_3OH \cdots HOCH_3$ featured an extended chain along the unit cell c axis (Figure 5). This one-dimensional chain is formed by $N-H \cdots O$ [$N2 \cdots O1 = 3.018(3)$ Å, $N1 \cdots O2 = 2.852(4)$ Å, and $N4 \cdots O1 = 3.052(4)$ Å] and $CH_3OH \cdots HOCH_3$ [$O1 \cdots O2 = 2.664(4)$ Å ($O-H \cdots O$); $C69 \cdots O2 = 3.064(6)$ Å ($C-H \cdots O$)] hydrogen-bonding interactions. Interchain interactions are largely van der Waals in nature because the close contact $C \cdots C$ distance between the adjacent chains is 3.459(4) Å. The observed hydrogen-bonding distances indicate moderate to fairly strong intermolecular interactions in the $H_2(TPP(Ph)_4Cl_4) \cdot 2(CH_3OH)$ structure, while similarly solvated $H_2(TPP(Ph)_4X_4)$ (X = CN, Br) structures showed very weak intermolecular interactions.[72] Geometrical and structural parameters of the porphyrin ring in these structures seem to suggest that the steric crowding is predominantly responsible for induced nonplanarity of the macrocycle.

Crystal structures of $Ni(TPP(Ph)_4(CN)_4) \cdot C_6H_{14} \cdot 0.5(C_2H_4Cl_2)$ and $Zn(TPP(Ph)_4Cl_4)(Py) \cdot C_2H_2Cl_4$ complexes were determined to elucidate the role of the divalent metal ion in the stereochemistry of the porphyrin skeleton. The crystallographic data of the complexes are listed in Table 1. An ORTEP diagram of $Ni(TPP(Ph)_4(CN)_4) \cdot C_6H_{14} \cdot 0.5(C_2H_4Cl_2)$ is shown in Figure 6a. The selected bond lengths and geometrical parameters of these porphyrin skeletons are listed in Table 3. The bond lengths and angles are comparable to that reported for the $Ni(TPP(Ph)_4(CN)_4Br_4) \cdot 2.5(C_2H_4Cl_2)$ complex.[60] The edge-on view of the Ni(II) complex shows con-

(72) Desiraju, G. R.; Steiner, T. *The Weak Hydrogen Bond in Structural Chemistry and Biology*; Oxford University Press: Oxford, U.K., 1999.
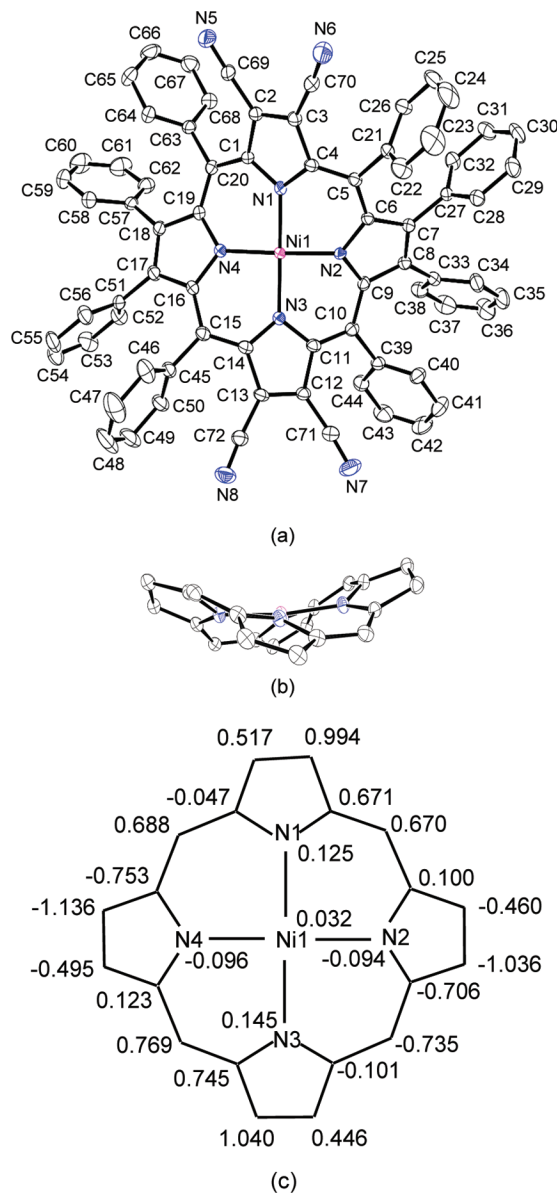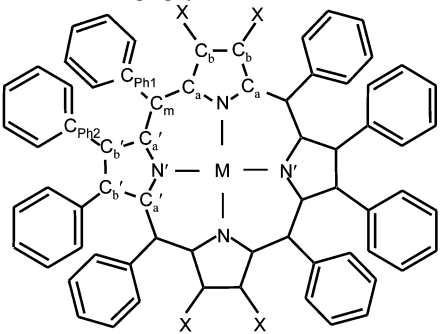
Figure 6. ORTEP diagrams of $Ni(TPP(Ph)_4(CN)_4) \cdot C_6H_{14} \cdot 0.5(C_2H_4Cl_2)$ complex. (a), top view and (b), side view (the solvate, phenyl, cyano and hydrogen atoms are not shown for clarity). Thermal ellipsoids are shown at 40% probability. (c) The displacements of the Ni(II) ion and the core atoms are shown in ångstrom units (esd's, 0.004 Å).

siderable nonplanarity of the porphyrin ring (Figure 6b). The Ni(II) ion is situated slightly above the mean plane by 0.032(4) Å. The pyrrole rings with electron-withdrawing β-cyano groups decrease the electron density on the nitrogen atoms, resulting in an elongation of the Ni$-$N bond distance, but interestingly, it is marginally shorter when compared to the Ni$-$N$'$ bond length for β-pyrroles bearing electron-donor phenyl groups (Table 3). These distances are less than that found in the more electron-deficient four-coordinated $Ni(TPP(CN)_4Br_4) \cdot 2.5(C_2H_4Cl_2)$ structure[60] ($Ni-N_{p(CN)} = 1.929(4)$ Å; $Ni-N_{p(Br)} = 1.911(4)$ Å). The nonplanar cores tend to show shorter Ni$-$N bond distances,[60] if the porphyrin pyrrole rings are substituted with electron-withdrawing groups, the basicity of these nitrogens tends to decrease, resulting in increased Ni$-$N bond distances. The marginal decrease in the Ni$-$N bond distance relative to Ni$-$N$'$ in the $Ni(TPP(Ph)_4(CN)_4) \cdot C_6H_{14} \cdot 0.5(C_2H_4Cl_2)$ complex

Table 3. Selected Mean Bond Lengths and Geometrical Parameters of Mixed Substituted Metalloporphyrins

M = Ni(II), X = CN, Ni(TPP(Ph)$_4$(CN)$_4$)•(C$_6$H$_{14}$)•0.5(C$_2$H$_4$Cl$_2$), **4**

M = Zn(II), X = Cl, Zn(TPP(Ph)$_4$Cl$_4$)(Py)•(C$_2$H$_4$Cl$_2$), **5**

	4	**5**
Bond Length (Å)		
M−N	1.882(3)	2.104(5)
M−N′	1.902(3)	2.051(4)
C$_a$−N	1.371(5)	1.370(4)
C$_a$′−N′	1.384(5)	1.374(4)
C$_a$−C$_b$	1.440(5)	1.449(6)
C$_a$′−C$_b$′	1.456(6)	1.455(6)
C$_b$−C$_b$	1.378(6)	1.349(6)
C$_b$′−C$_b$′	1.363(6)	1.366(6)
C$_a$−C$_m$	1.402(6)	1.405(6)
C$_a$′−C$_m$	1.394(6)	1.410(6)
Bond Angle (deg)		
M−N−C$_a$	125.2(3)	121.7(2)
M−N′−C$_a$′	126.1(3)	125.9(2)
C$_a$−N−C$_a$	108.3(3)	108.8(3)
C$_a$′−N′−C$_a$′	106.2(3)	106.9(3)
C$_a$−C$_m$−C$_a$	119.8(3)	124.1(3)
N−C$_a$−C$_m$	124.7(3)	124.0(1)
N′−C$_a$′−C$_m$	122.4(3)	124.4(1)
N−C$_a$−C$_b$	108.6(3)	107.8(4)
N′−C$_a$′−C$_b$′	109.7(3)	109.6(2)
C$_b$−C$_a$−C$_m$	126.0(3)	128.0(4)
C$_b$′−C$_a$′−C$_m$	127.0(4)	125.9(4)
C$_a$−C$_b$−X	129.3(4)	129.0(1)
C$_a$′−C$_b$′−C$_{ph2}$	127.2(4)	127.2(4)
(N−M−N)$_{opp}$	173.0(14)	161.2(4)
(N−M−N)$_{adj}$	90.2(14)	88.5(3)
Dihedral Angle Relative to the Mean Plane (deg)		
meso-phenyl	57.5(2)	57.0(2)
β-phenyl	68.5(1)	61.4(2)
pyrrole (X)	27.8(2)	19.8(2)
pyrrole (Ph)	30.7(2)	24.9(2)

is perhaps due to contraction of the porphyrin core rather than electronic effects of the pyrrole nitrogens. It was reported earlier that the Ni−N distances were less in four-coordinated low-spin Ni(II) porphyrins and known to exhibit distortion of the porphyrin skeleton.[73] It can be seen that the (N−Ni−N)$_{adj}$ angle is close to 90°, while the (N−Ni−N)$_{opp}$ angle deviates signifi-

(73) (a) Veyarath, M.; Ramassuel, R.; Marchon, J. C.; Turovska-Tyrk, I.; Scheidt, W. R. *New J. Chem.* **1995**, *19*, 1199. (b) Hobbs, J. D.; Majumder, S. A.; Luo, L.; Sickelsmith, G. A.; Auirke, J. M. E.; Medforth, C. J.; Smith, K. M.; Shelnutt, J. A. *J. Am. Chem. Soc.* **1994**, *116*, 3261. (c) Barkigia, C. M.; Renner, M. W.; Furenlid, L. R.; Medforth, C. J.; Smith, K. M.; Fajer, J. *J. Am. Chem. Soc.* **1993**, *115*, 3627. (d) Scheidt, W. R. In *The Porphyrins*; Dolphin, D., Ed.; Academic Press: New York, 1978; Vol. 3, p 463. (e) Cullen, D. L.; Meyer, E. F., Jr. *J. Am. Chem. Soc.* **1974**, *96*, 2095. (f) Brennan, T. D.; Scheidt, W. R.; Shelnutt, J. A. *J. Am. Chem. Soc.* **1988**, *110*, 3919. (g) Kratky, C.; Waditschatka, R.; Angst, C.; Johansen, J. E.; Plaquevent, J.; Schreiberg, J.; Eschenmoser, A. *Helv. Chim. Acta* **1985**, *68*, 1312.

cantly from 180°, indicating distorted square-planar geometry around the Ni(II) ion (Table 3). The observed structural features in Ni(TPP(Ph)$_4$(CN)$_4$)•C$_6$H$_{14}$•0.5(C$_2$H$_4$Cl$_2$) indicate the low-spin complex, and such a feature was previously known for highly substituted four-coordinated Ni(II) porphyrins such as 2,3,7,8,12,13,17,18-octabromo-5,10,15,20-tetramesitylporphinato nickel(II), 2,3,7,8,12,13,17,18-octabromo-5,10,15,20-tetrakis(pentafluorophenyl) porphinato nickel(II), and 2,3,7,8, 12,13,17,18-octachloro-5,10,15,20-tetraphenylporphinato nickel(II) complexes.[33a] The average C$_b$−C$_b$ (1.378(6) Å) bond distance is marginally longer than C$_b$′−C$_b$′ (1.363(6) Å), and these distances are greater than the corresponding [1.368(7) and 1.342(7) Å] data reported for the similarly functionalized NiTPP(CN)$_4$Br$_4$•2.5(C$_2$H$_4$Cl$_2$) complex. The average C≡N distance (1.146(6) Å) is greater in the present complex than in the corresponding reported four-coordinated Ni(II) complex (1.064(15) Å).[60]

The mean plane deviation of the core atoms in Ni(TPP-(Ph)$_4$(CN)$_4$)•C$_6$H$_{14}$•0.5(C$_2$H$_4$Cl$_2$) are shown in Figure 6c. There is significant distortion of the 24-atom core in the Ni(II) complex (Table 3). The nonplanarity of the porphyrin ring is also evident from the deviation of the β-pyrrole and the meso-carbons from the mean plane (Table 3, Figure 6c). The meso-phenyl groups showed a lesser dihedral angle when compared to the β-pyrrole phenyl groups (Table 3). The pyrrole rings are tilted alternatively up and down with an average dihedral angle of 29.3(2)° relative to the mean plane of the porphyrin. The corresponding six coordinated Ni(TPP(Ph)$_4$(CN)$_4$)(Py)$_2$•(Py)[62] structures feature nearly planar geometry with the expansion of the porphyrin core and elongation of the Ni−N bond lengths in the equatorial plane.[62] In addition, the average dihedral angle formed by the phenyl groups to the porphyrin mean plane was reported to be 80.8(5)°. In the case of the Ni(TPP(Ph)$_4$(CN)$_4$)• C$_6$H$_{14}$•0.5(C$_2$H$_4$Cl$_2$) complex, the short intramolecular contact distance for (CN)N···C (meso-o-phenyl carbon) was found to be 3.231(3) Å. Intermolecular interactions in this complex indicate an unusual CN(N)···porphyrin with a short contact distance of N6···C17 = 3.072(7) Å. The porphyrin solvate (C$_2$H$_4$Cl$_2$) is influenced by weak C−H···Cl (C23···Cl1 = 3.400(9)) Å interactions. This suggests the possible influence of the weak intermolecular interactions on the nonplanar conformation of the porphyrin.

An ORTEP diagram of the Zn(TPP(Ph)$_4$Cl$_4$)(Py)• (C$_2$H$_4$Cl$_2$) complex is shown in Figure 7a. The selected bond lengths and angles for both the Zn(II) complexes are listed in Table 3. In the equatorial plane, the Zn−N bond distance is longer along the chloro-substituted pyrroles, while it is shorter along the phenyl-substituted pyrroles. This indicates the decreased electron density of the pyrrole nitrogens bearing chloro substituents relative to the pyrroles with the electron-donor β-phenyl groups. The Zn−N distances observed in the equatorial plane are comparable to that reported for five-coordinated Zn(TPP(Ph)$_4$Br$_4$)(CH$_3$OH)•CH$_3$OH[62] and Zn(TPPBr$_4$)(CH$_3$OH)•DMF[64] structures. Interestingly, the C$_b$−C$_b$ bond length is marginally shorter in pyrroles with chloro groups in contrast to the C$_b$′−C$_b$′ distances in pyrroles

Figure 7. ORTEP diagrams of the ZnTPP(Ph)$_4$Cl$_4$(Py)·(C$_2$H$_4$Cl$_2$) complex. (a) Top view (hydrogens and minor disordered pyridyl group are not shown) and (b) side view (solvate, phenyls, chloro, and hydrogen atoms are omitted for clarity). Thermal ellipsoids are shown at 40% probability. (c) The displacements of the Zn(II) ion and core atoms from the mean plane in ångstrom units (esd's 0.004 Å).

with β-phenyl groups (Table 3). This is perhaps due to the influence of steric crowding induced by the peripheral substituents rather than electronic factors.

The equatorial nitrogens are situated almost in a square-planar conformation within an average deviation of ±0.063(3) Å from the mean plane. The Zn(II) ion is situated about 0.368 (4) Å from the plane of the four nitrogen atoms with a fairly short axial (Zn–N$_{pyridine}$) distance of 2.145(4) Å. The axially ligated pyridine shows two disordered positions bent significantly toward the mean plane with (N4–Zn1–N5) dihedral angles of 58.4(2)° and 60.7(3)° (Figure 7b). A similar Zn–N$_{pyridine}$ distance (2.144(9) Å) was reported for

Table 4. Comparison of Selected Mean Bond Lengths and Angles of the Cores in H$_2$(TPP(Ph)$_4$X$_4$) (X = CN, Cl) and Their Metal Complexes

	H$_2$(TPP(Ph)$_4$-(CN)$_4$)	Ni(TPP(Ph)$_4$-(CN)$_4$)	H$_2$(TPP(Ph)$_4$-Cl$_4$	Zn(TPP(Ph)$_4$-Cl$_4$)(Py)
Bond Length (Å)				
M–N		1.892(3)		2.078(4)
C$_a$–N	1.367(5)	1.378(5)	1.370(4)	1.372(3)
C$_b$–C$_b$	1.379(5)	1.371(6)	1.363(5)	1.358(6)
C$_a$–C$_b$	1.447(5)	1.448(5)	1.448(5)	1.452(6)
C$_a$–C$_m$	1.407(5)	1.398(6)	1.411(5)	1.408(6)
r.m.s.[a]	0.508	0.632	0.687	0.530
Bond Angle (deg)				
(N–M–N)$_{adj}$		90.2(14)		88.5(3)
(N–M–N)$_{opp}$		173.0(14)		161.1(5)
M–N–C$_a$		125.7(3)		123.8(2)
C$_a$–N–C$_a$	109.1(3)	107.3(3)	109.1(3)	107.9(3)
N–C$_a$–C$_b$	108.3(3)	109.2(3)	107.9(3)	108.7(3)
N–C$_a$–C$_m$	125.2(3)	123.6(3)	124.0(3)	124.2(2)
C$_a$–C$_m$–C$_a$	124.0(3)	119.8(3)	122.3(3)	124.1(4)
C$_b$–C$_a$–C$_m$	126.5(3)	126.5(3)	128.1(3)	127.0(4)
Average Dihedral Angle (deg)				
phenyl	57.9(3)	63.0(2)	48.3(2)	59.2(2)
pyrrole	22.1(2)	29.3(2)	32.6(3)	22.4(2)
Distance (Å)				
N···N	4.044(3)	3.760(4)	4.245(4)	4.169(3)
N'···N'	4.227(3)	3.794(3)	4.122(4)	4.026(4)

[a] r.m.s., root-mean-square displacement of the core atom (in ångstroms) from the 24-atom core.

the five-coordinated nonplanar 2,3,7,8,12,13,17,18-octamethyl-5,10,15,20-tetraphenylporphinato zinc(II) pyridine solvate.[28] In the equatorial plane, the (N–Zn–N)$_{opp}$ angles significantly deviate from 180°, while the (N–Zn–N)$_{adj}$ angle is approximately close to 90° (Table 3). The displacement of β-pyrrole and *meso*-carbons indicates that the stereochemical features of the 24-atom core in Zn(TPP-(Ph)$_4$Cl$_4$) are significantly altered (Table 3) in contrast to that observed for the H$_2$(TPP(Ph)$_4$Cl$_4$)·2(CH$_3$OH) structure. The adjacent chloro groups deviate from each other and from the pyrrole ring mean plane by 0.045(2) Å. Similarly, the phenyl carbon (C27, C33, C51, and C57) atoms attached to the β-pyrrole positions deviate from the adjacent phenyl carbon by < 0.059(2) Å. The short intramolecular contact distance between the β-Cl and the adjacent *meso-o*-phenyl carbon is 3.193(4) Å.

To elucidate the extent of distortion of the macrocyclic ring by the core metal ions, the average bond lengths and geometrical parameters of Ni(TPP(Ph)$_4$(CN)$_4$)·C$_6$H$_{14}$·0.5-(C$_2$H$_4$Cl$_2$) and Zn(TPP(Ph)$_4$Cl$_4$)(Py)·C$_2$H$_4$Cl$_2$ were compared with their corresponding free base structures (Table 4). The metal complexes showed interesting structural differences compared to their free base porphyrin derivatives. It is known that the porphyrin ring is sensitive to the size of the divalent core metal ion. In-plane asymmetric distortion is anticipated to decrease with the incorporation of the Ni(II) ion, which results in an increase in C$_a$–N and C$_a$–C$_m$ bond distances and a decrease in C$_a$–N–C$_a$ and N–C$_a$–C$_m$ angles in contrast to its free base porphyrin structure.[67,17c] The NiOPP(CN)$_4$ structure shows a lengthening of C$_a$–N and a marginal decrease in C$_a$–C$_m$ bond distances, but decreases in C$_a$–N–C$_a$ and C$_a$–C$_m$–C$_a$ angles were observed relative to those of the H$_2$(TPP(Ph)$_4$(CN)$_4$) structure (Table 4). With the increase in size of the divalent metal ion, there is an increase in M–N and C$_a$–C$_m$ bond distances with shorter

Table 5. Normal-Coordinate Decomposition Analysis of Free Base Porphyrins and Their Metal Complexes[a]

					out-of-plane displacements (Å)						
	D_{oop}	B_{2u}, sad	B_{1u}, ruf	A_{2u}, dom	$Eg(x)$, wav(x)	$E_g(y)$, wav(y)	A_{1u}, prop	sum	sad/sum (%)	ruf/sum (%)	dom/sum (%)
1	2.4628	2.3884	−0.5136	−0.2389	0.0771	0.1801	−0.0382	3.4363	69.5	14.9	6.9
2	3.3055	−3.3010	0.0127	−0.1690	−0.0328	−0.0003	0.0071	3.5229	93.7	0.4	4.8
3	3.8113	3.8070	0.1281	−0.0976	0.0518	−0.0566	0.0265	4.1676	91.3	3.1	2.3
4	3.0910	−2.3478	−2.0045	0.0617	0.1163	−0.0501	0.0662	4.6466	50.5	43.1	1.3
5	2.5970	2.5857	−0.0442	−0.1727	−0.0520	−0.1515	−0.0353	3.0414	85.0	1.5	5.7

					in-plane-displacements (Å)						
	D_{ip}	B_{2g} (m-str)	B_{1g} (N-str)	$E_u(x)$ (trn)	$E_u(y)$ (trn)	A_{1g} (bre)	A_{2g} (rot)	sum	B_{2g}/ sum (%)	B_{1g}/ sum (%)	A_{1g}/ sum (%)
1	0.3074	−0.0733	−0.2540	−0.0254	0.0229	−0.1508	−0.0263	0.5527	13.3	45.9	27.3
2	0.5928	0.0046	0.3512	−0.0053	0.0112	−0.4774	0.0036	0.8533	0.5	41.2	55.9
3	0.7673	0.0358	0.0005	−0.0206	−0.0130	−0.7656	0.0281	0.8636	4.1	∼0	88.7
4	0.8565	0.0334	0.0830	0.0560	−0.0479	−0.8479	0.0354	1.1036	3.0	7.5	76.8
5	0.2753	0.0179	−0.1843	0.0287	−0.0158	−0.2008	0.0110	0.4585	3.9	40.2	43.8

[a] **1**, $H_2(TPP(Ph)_4(CN)_4)$; **2**, $H_2(TPP(Ph)_4Cl_4)$; **3**, $H_2(TPP(Ph)_4Br_4)$; **4**, $Ni(TPP(Ph)_4(CN)_4)$; **5**, $Zn(TPP(Ph)_4Cl_4)(Py)$.

C_a−N bond lengths. Further, C_a−N−C_a and C_a−C_m−C_a angles tend to increase, and the M−N−C_a angle decreases with the reduction in nonplanarity of the 24-atom core.[1,3] Interestingly, the $Ni(TPP(Ph)_4(CN)_4) \cdot C_6H_{14} \cdot 0.5(C_2H_4Cl_2)$ complex exhibited an enhanced dihedral angle for the phenyl and the pyrrole rings relative to its free base porphyrin structure. The increase in distortion of the macrocyclic ring in the $Ni(TPP(Ph)_4(CN)_4)$ complex is reflected in the root-mean-square deviation of the core atom and pyrrole dihedral angle in contrast to its free base porphyrin (Table 4). In the $Zn(TPP(Ph)_4Cl_4)(Py) \cdot (C_2H_4Cl_2)$ complex, the mean bond lengths of the 24-atom core are comparable to its free base structure; however, they showed significant differences in some bond angles. For example, C_a−N and C_a−C_m bond distances are similar, but there is a decrease in C_a−N−C_a and an increase C_a−C_m−C_a angles relative to that observed in the $H_2(TPP(Ph)_4Cl_4) \cdot 2(CH_3OH)$ structure (Table 4). There is a decrease in nonplanarity of the porphyrin ring in the Zn(II) complex. The N···N separations in $Ni(TPP(Ph)_4(CN)_4)$ and $Zn(TPP(Ph)_4Cl_4)$ exhibited contraction of the cores relative to their corresponding free base structures (Table 4). The extent of contraction of the (N_4) core is more dramatic in the Ni(II) complex when compared to the Zn(II) complex. As expected, the pyrrole groups showed increased and decreased dihedral angles in the Ni(II) and Zn(II) complexes, respectively, relative to their free base structures. This is reflected by the root-mean-square displacement of the core atoms. The average dihedral angles made by the phenyl groups relative to the porphyrin ring mean plane are increased significantly in $Ni(TPP(Ph)_4(CN)_4)$ and $Zn(TPP(Ph)_4Cl_4)(Py) \cdot (C_2H_4Cl_2)$ structures relative to their corresponding free base structures (Table 4).

To determine the different degree of contribution from the lowest-energy out-of-plane displacements (D_{oop}) and in-plane displacements (D_{ip}) of the free base porphyrin macrocycle, crystal structures of the 24-atom core $(C_{20}N_4)$ were examined by normal-coordinate structure decomposition (NSD) analysis.[2c,74] Table 5 lists the contributions from the different degrees of saddling (sad, B_{2u}), ruffling (ruf, B_{1u}), doming (dom, A_{2u}), waving (wav(x),wav(y), E_g), and propellering (prop, A_{1u}) of the distortion of the macrocycle. Both total distortion D_{oop} and the core elongation of the macrocyclic ring vary in the order $H_2(TPP(Ph)_4(CN)_4) < H_2(TPP(Ph)_4Cl_4) < H_2(TPP(Ph)_4Br_4)$. Thus, in the series, $H_2(TPP(Ph)_4(CN)_4) \cdot 3(C_2H_4Cl_2)$ shows the least nonplanarity and least elongation of the N_4H_2 core. The free base structures, $H_2(TPP(Ph)_4X_4)$ (X = CN, Cl, Br), showed contributions mainly from saddling with varying degrees of ruffling and dome conformations, but the $H_2(TPP(Ph)_4(CN)_4)$ structure features additional minor wav(x),wav(y) contributions. The NSD calculations show that the saddling increases sharply from $H_2(TPP(Ph)_4(CN)_4)$ to $H_2(TPP(Ph)_4Cl_4)$ with the decrease in ruffling of the ring. For the $H_2(TPP(Ph)_4Br_4)$ structure, a slight decrease in saddling with a small increment in ruffling was observed in contrast to that of the $H_2(TPP(Ph)_4Cl_4)$ structure. In-plane displacements of the free base porphyrins are also listed in Table 5. The N-breathing (A_{1g}) and N-stretching (B_{1g}) contribute significantly to the in-plane displacement of the core atoms. However, the m-stretching (B_{2g}) contributes minimally for $H_2(TPP(Ph)_4X_4)$ (X = Cl, Br) and moderately for $H_2(TPP(Ph)_4(CN)_4)$. The other displacements [E_u (translation), A_{2g} (rotation)], contribute very minimally, mainly to in-plane displacements. As suggested previously,[74a] B_{1g}, B_{2g}, and A_{1g} contribute for in-plane displacements since they are energetically favorable when compared to other displacements. Nearly planar free base porphine (H_2P) and octaethylporphyrin (H_2OEP) structures are reported to be very small for in-plane and out-of-plane displacements.[2b] NSD calculations on the 2,3,7,8,12,13,17, 18-octaethyl-5,10,15,20-tetraphenylporphinato nickel(II) exhibited in-plane and out-of-plane displacements with predominantly saddled distortion of the macrocyclic ring,[2d,3,16] and the magnitudes of the displacements are similar to that observed for the $H_2(TPP(Ph)_4Br_4) \cdot 2(THF) \cdot 1.5(CH_3OH)$ structure.

The metalation of $H_2(TPP(Ph)_4X_4)$ (X = Br,[62] Cl) by the Zn(II) ion exhibited decreased nonplanarity of the ring, and a similar trend was observed in the structure of five-coordinated complex 2,3,7,8,12,13,17,18-octaethyl-5,10,15,20-tetraphenylporphinato zinc(II) methanol.[28] The data from the

(74) (a) Jentzen, W.; Ma, J.-Ma.; Shelnutt, J. A. *Biophys. J.* **1998**, *74*, 753. (b) Sun, L.; Jentzen, W.; Shelnutt, J. A. The Normal Coordinate Structural Decomposition Engine. http://jasheln.unm.edu /jasheln/content/nsd/NSDengine (accessed Mar 2009).

NSD calculations on the porphyrin ring in $Ni(TPP(Ph)_4(CN)_4) \cdot C_6H_{14} \cdot 0.5(C_2H_4Cl_2)$ and $Zn(TPP(Ph)_4Cl_4)(Py) \cdot C_2H_4Cl_2$ complexes are listed in Table 5. The geometry of the complex (Figure 6) and the data in Table 5 suggest that the degree of saddling and ruffling is approximately similar in the $Ni(TPP(Ph)_4(CN)_4) \cdot C_6H_{14} \cdot 0.5(C_2H_4Cl_2)$ complex, while $Zn(TPP(Ph)_4Cl_4) \cdot (C_2H_4Cl_2)$ predominantly (Figure 7) shows saddling with a very minimal doming contribution. Moreover, the extent of saddling is decreased in the metal complex relative to the corresponding free base porphyrins. The reported NSD analysis on the four-coordinated $Ni(TPP(CN)_4Br_4)$ complex indicated predominant saddling (sad = 3.068 Å) with very moderate ruffling (ruf = 0.205 Å) of the macrocycle.[60] $Ni(TPP(Ph)_4(CN)_4)$ shows a major in-plane displacement contribution from the *N*-breathing (A_{1g}) mode, and it is considerably less in the parent $H_2(TPP(Ph)_4(CN)_4) \cdot 3(C_2H_4Cl_2)$ structure. $Zn(TPP(Ph)_4Cl_4)(Py) \cdot C_2H_4Cl_2$ exhibits decreased A_{1g} and B_{1g} displacements relative to the $H_2TPP(Ph)_4Cl_4$ structure. The observed out-of-plane displacement in $Ni(TPP(Ph)_4(CN)_4) \cdot C_6H_{14} \cdot 0.5(C_2H_4Cl_2)$ shows the role of the shape of the substituent Ph versus the Br group, as in the $Ni(TPP(CN)_4Br_4)$ complex. Previous structures of partially substituted free base porphyrins, $H_2(TPPR_4)$ (R = C_6H_5, CH_3, and Br), feature nearly planar geometry of the macrocyclic ring. Crystal structures of highly substituted porphyrins showed a nonplanar conformation induced by the steric crowding of the peripheral substituents.[1] As reported, the size and number of substituents alter the extent of steric crowding around the porphyrin periphery, and β-octasubstituted MTPPs produced varying degrees of nonplanarity.[1] Mixed dodecasubstituted porphyrins, 2,3,12,13-tetramethyl-5,7,8,10,15,17,18,20-octaphenylporphinato copper(II) dichloroform solvate and 2,3,12,13-tetrabromo-5,7,8,10,15,17,18,20-octaphenylporphinato zinc(II) dimethanol solvate structures featured nonplanar distortion of the porphyrin macrocycle.[62]

Conclusions

The influence of mixed substituents on the stereochemistry of the porphyrin skeleton has been examined by changing the size of the X group in $H_2(TPP(Ph)_4X_4)$ (X = CN, Cl, Br) derivatives. The macrocyclic ring shows considerable distortion. The extent of nonplanarity increases with the size of the X groups, and it follows the order CN < Cl < Br. Interestingly, the average core (N_4H_2) sizes in these mixed substituted free base porphyrins follow the trend $H_2(TPP(Ph)_4(CN)_4) < H_2(TPP(Ph)_4Cl_4) < H_2(TPP(Ph)_4Br_4)$. Furthermore, normal-coordinate decomposition analysis of the free base porphyrin structures, $H_2(TPP(Ph)_4X_4)$ (X = Cl, Br), showed predominantly saddle-shaped geometry, while the $H_2(TPP(Ph)_4(CN)_4)$ structure exhibited a combination of mostly saddled and ruffled conformations. The crystal structure of the $Zn(TPP(Ph)_4Cl_4)(Py) \cdot C_2H_4Cl_2$ exhibited distorted square-pyramidal geometry around the Zn(II) ion, and the $Ni(TPP(Ph)_4(CN)_4) \cdot C_6H_{14} \cdot 0.5(C_2H_4Cl_2)$ complex features nearly square-planar geometry around the Ni(II) ion. As observed from the NSD analysis, the macrocyclic ring in $Zn(TPP(Ph)_4Cl_4)(Py)$ exhibited less nonplanarity relative to its free base structure, which predominantly showed saddled-shaped geometry, while a combination of saddling and ruffling was observed in the $Ni(TPP(Ph)_4(CN)_4)$ structure. The nonplanarity of the $Ni(TPP(Ph)_4(CN)_4)$ was attributed to the steric crowding and contraction of the porphyrin core combined with the possible weak intermolecular interactions. The varying nonplanar distortions in free base porphyrins showed the effect of steric crowding by the mixed substituents on the conformational flexibility in these systems.

Supporting Information Available: Atomic positional parameters, bond lengths, angles, anisotropic thermal parameters, and a crystallographic information file (CIF) for all of the structures are available. This material is available free of charge via the Internet at http://pubs.acs.org.

IC801618M